Chinese Chemical Letters 32 (2021) 3852–3856

Contents lists available at ScienceDirect

Chinese Chemical Letters

journal homepage: www.elsevier.com/locate/cclet

Communication

Rapid formation of metal–monophenolic networks on polymer membranes for oil/water separation and dye adsorption

Jia-Lu Shen[a], Bing-Pan Zhang[a], Di Zhou[a], Zhi-Kang Xu[a], Ling-Shu Wan[a,*]

MOE Key Laboratory of Macromolecular Synthesis and Functionalization, Key Laboratory of Adsorption and Separation Materials & Technologies of Zhejiang Province, Department of Polymer Science and Engineering, Zhejiang University, Hangzhou 310027, China

ARTICLE INFO

Article history:
Received 25 March 2021
Revised 26 April 2021
Accepted 14 May 2021
Available online 24 May 2021

Keywords:
Metal–phenolic networks
Polymer membrane
Surface coating
Oil/water separation
Dye adsorption

ABSTRACT

Surface deposition based on metal-phenolic networks (MPNs) has received increasing interest in recent years. The catechol structure is generally considered to be essential to the formation of MPNs. Our most recent results have demonstrated that some kinds of monophenols can form MPNs on substrate surfaces. Herein, we report a fast and effective surface-coating system based on the coordination of 3-(4-hydroxy-3-methoxyphenyl)-2-propenoic acid, a kind of monophenol, with Fe^{3+}. Compared with other metal ions such as Cu^{2+} and Ni^{2+}, Fe^{3+} with stronger electron acceptability can coordinate with the monophenol more strongly to form MPNs, and moreover, the deposition time significantly decreases to 40 min from generally 24 h. It is demonstrated that the deposition process is controlled by the coordination, Fe^{3+} hydrolysis, and deprotonation of the monophenol. The coatings endow substrates such as polypropylene microfiltration membrane with underwater superoleophobicity, which can be applied in oil/water separation with high separation efficiency and great long-term stability. In addition, the coated membranes are positively charged and thus are useful in selective adsorption of dyes. The present work not only provides a novel, fast, and one-step deposition method to fabricate MPNs, but also demonstrates that the fabrication efficiency of monophenol-based MPNs is comparable with that of polyphenol-based MPNs.

Surface coatings with multifunctional properties have attracted great attention in the chemical, physical, and biomedical sciences [1–4]. To form surface coatings on different materials, various methods have been studied including surface grafting [5], dip coating [6], chemical vapor deposition [7], electrospinning [8], layer-by-layer deposition [9,10], atomic layer deposition [11], polydopamine (PDA) deposition [12–15] and metal-phenolic networks (MPNs) formation [16–18]. For example, inspired by the adhesive proteins in mussels, Lee *et al*. reported thin and surface-adherent PDA coatings [19]. This method shows some advantages over other techniques, such as substrate independence and time-saving processes [12]. High cost, dark color and relatively low stability were the main drawbacks of PDA coatings for practical applications, and they have been improved to some extent in recent years.

MPNs [16–18] are an emerging class of materials which are based on metal–ligand coordination. Benefiting from diverse combinations of metal ions and phenolic ligands, time-saving process, and pH-responsive property, MPNs show potential applications in drug delivery [20], energy storage [21], catalysis [22], membrane separation [23], rewritable paper [24], elastomers [25] and self-healing hydrogels [26]. There are several studies reported the deposition of diverse MPNs on various substrates by simply immersing the substrates into the mixture solution of metal ions and phenols. The formation mechanism is commonly recognized as follows: phenols firstly adhere onto the surface of substrates through hydrogen or hydrophobic interaction, π-π conjugation, and other interaction force, and then are cross-linked by transition metal ions [16,27].

Phenols are widely found in plants, and many of them are commercially available as well as cheap [28,29]. Among abundant phenols, tannic acid that has twenty five phenolic hydroxyl groups is most commonly used to fabricate MPNs, and the catechol structure is always considered to be essential for the successful construction of uniform coatings [30–34]. Recently, it has been found that some kinds of monophenols such as juglone, can form surface coatings alone or form MPNs on various substrate surfaces [35–38]. As an example, 3-(4-hydroxy-3-methoxyphenyl)-2-propenoic acid (ferulic acid, FA), which has only one phenolic hydroxyl group (Fig. 1a), can coordinate with Cu^{2+} ions and form MPNs on a wide range of inorganic and organic substrates [37]. However, the FA/Cu^{2+} system is time-consuming which requires generally 24 h deposition, and the

* Corresponding author.
E-mail address: lswan@zju.edu.cn (L.-S. Wan).

https://doi.org/10.1016/j.cclet.2021.05.023
1001-8417/

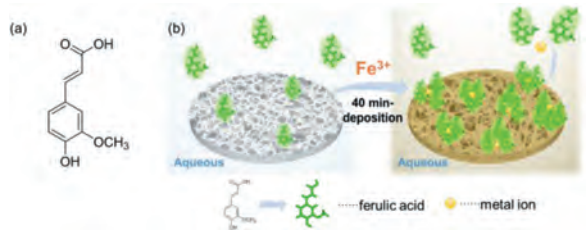

Fig. 1. (a) Chemical structure of 3-(4-hydroxy-3-methoxyphenyl)-2-propenoic acid (FA) and (b) schematic illustration of the FA/Fe^{3+} deposition process.

use of Cu^{2+} may cause environmental and health hazards, limiting further applications of the resultant MPNs.

In this communication, we report that the Fe^{3+} ions with stronger electron acceptability than Cu^{2+} are conducive to form MPNs with FA, and significantly shorten deposition time from about 24 h to only 40 min (Fig. 1b). The coatings endow substrates such as polypropylene microfiltration membrane (PPMM) with positive surface charge and underwater superoleophobicity, which enables applications in anion dyes adsorption and oil/water separation with high separation efficiency, high flux, and great long-term stability. This work provides a novel, fast, and one-step deposition method to fabricate monophenol-based MPNs, and demonstrates the potential applications of microporous membranes coated with MPNs.

We chose hydrophobic PPMM as a typical substrate to study the formation of MPNs from FA and some metal ions. In the one-step deposition process, FA molecules adhere to the substrate surface via hydrophobic interaction and π-π conjugation [39,40]. Meanwhile, the oxygen atoms of phenolic hydroxyl group, methoxyl group, and carboxyl group donate their lone pair electrons to transition metal ions to form coordination bonds and hence cross-linked networks with metal ions as the cross-linker [27].

The coordination between transition metal ions and ligands can be guided by hard and soft acids and bases (HSAB) theory [41,42]. According to the HSAB theory, hard Lewis acids prefer binding with hard Lewis bases, and *vice versa*. The hardness of a Lewis acid depends on electron acceptability of the metal ion, which can be quantified by ionization potential. As shown in Fig. 2a and Table S1 (Supporting information), the order of hardness is $Fe^{3+} > Cu^{2+} > Ni^{2+} > Zn^{2+}$, of which Fe^{3+} is a hard acid and the others are borderline acids. FA can be considered as a hard base for its carboxyl group and phenolic hydroxyl group. Therefore, it is predictable that FA prefers to coordinate with hard acids [41]. To prove the speculation mentioned above, the influence of different kinds of metal ions was investigated.

The ATR-FTIR spectrum of FA/Fe^{3+}-coated PPMM displays characteristic C=O, benzene ring, and C–O bands at around 1650~1600 cm^{-1}, 1510 cm^{-1}, and 1278 cm^{-1}, respectively, revealing the deposition of FA (Fig. 2b) [37]. The same signals are observed for FA/Cu^{2+}-coated PPMM, but the intensity of the peaks is much weaker. When Ni^{2+} or Zn^{2+} or no metal ions is used, these signals cannot be observed. The stronger characteristic bands from FA in the spectrum of FA/Fe^{3+} than others suggest the higher FA content [42]. EDX results (Table S2 and Fig. S1 in Supporting information), photographs (Fig. 2b), UV-vis spectra (Fig. S2 in Supporting information), and FESEM images (Fig. S3 in Supporting information) also confirm effective and homogenous deposition of FA/Fe^{3+}, indicating that the coordination ability between FA and Fe^{3+} is stronger than the others. The solution becomes turbid immediately after mixing FA with Fe^{3+} (Fig. S4 in Supporting information), which means rapid formation of FA/Fe^{3+} coordination complexes. The FA/Fe^{3+} solution gets more turbid in the first hour, and the turbidity shows no obvious increase with the further elongation of time, demonstrating that the coordination and de-coordination between FA and Fe^{3+} has reached a balance after 1 h. However, the FA/Cu^{2+} solution is transparent at first and the turbidity increases slowly with time, indicating the poor coordination capability between FA and Cu^{2+}. As for FA/Zn^{2+} and FA/Ni^{2+}, the solutions keep clear and transparent even after 6 h.

Since the -OH and –COOH groups of FA are hydrophilic, the surface deposition is also a hydrophilization process. Dynamic water contact angle results show that the nascent PPMM has a stable water contact angle of 140° and the PPMMs treated by FA, FA/Ni^{2+}, and FA/Zn^{2+} remain hydrophobicity (Fig. 2c). After deposited with FA/Cu^{2+}, the water contact angle of the membrane decreases to ~90°. The FA/Fe^{3+}-coated PPMM can exhibit superhydrophilicity, on which water droplets fully spread out in 1 s.

To achieve fast and uniform formation of FA/Fe^{3+} MPNs and hydrophilization *via* the one-step deposition process, some factors relating to the deposition including pH of buffer solutions, mass ratio of FA to Fe^{3+}, and deposition time were investigated using PPMM as a typical substrate. As shown in Fig. S5a (Supporting information), the hydrophilicity of the coated PPMMs increases first and then deceases with pH values. At pH 4.0, 7.0, and 8.0, the water contact angles of the coated PPMMs are larger than 40°, which reduce to ~30° when pH is 5.0. The coated PPMM displays good hydrophilicity at pH 6.0, however the resulted MPN is not much uniform (Fig. S6a in Supporting information). As for the influence of the mass ratio of FA to Fe^{3+}, with the increase of $FeCl_3$•$6H_2O$ concentration from 2:0.5 to 2:8, the membrane surface becomes increasingly hydrophilic; and water droplets penetrate into the membrane completely in 1 s when the ratio reaches 2:8 (Fig. S5c in Supporting information). UV-vis (Figs. S5b and d in Supporting information) and EDX results (Tables S3 and S4 in Supporting information) are consistent with those of water contact angles. The influence of deposition time has also been studied. After only 20 min of deposition, the water contact angle obviously decreases to ~70° from ~140°; and deposition for 40 min leads to superhydrophilic membrane surface (Fig. S5e in Supporting information). The required deposition time is much shorter than FA/Cu^{2+} system.

The influence of pH and mass ratio is the result of some complicated processes including Fe^{3+} hydrolysis, FA deprotonation, and FA/Fe^{3+} coordination. High pH and Fe^{3+} concentration facilitate the formation of insoluble iron hydroxide species, which inhibit the coordination between FA and Fe^{3+}. However, high pH can also promote the deprotonation of phenolic hydroxyl groups and carboxyl groups of FA molecules, which will improve the electron donating ability of oxygen atoms and thus promote coordination [30,43,44]. At pH 5.0 and a mass ratio of 2:8, the suppression of hydrolysis of Fe^{3+} and the deprotonation of hydroxyl groups and carboxyl groups reach a balance, corresponding to an optimal state. The coordination process is rather quick, and the MPNs can be effectively formed in 40 min to realize superhydrophilicity of PPMM. When the deposition time is longer than 40 min, there is little difference in surface hydrophilicity of the modified membranes (Fig. S5e in Supporting information). Considering that a shorter deposition time is important for practical applications, we chose 40 min as the optimal deposition time in the following experiments unless otherwise indicated.

SEM and XPS were used to characterize surface morphology and chemical composition of the MPN coatings. The nascent PPMM is microporous, and its three-dimensional structure produces micro-sized protrusions on the surface (Fig. 2d and Fig. S7 in Supporting information). As for the FA/Fe^{3+}-coated PPMM, in addition to the micro surface structure, the membrane surface is covered by numerous nano-sized particles induced by the deposition (Fig. 2e) although the membrane thickness changes little before and after the deposition (Fig. S7 in Supporting information). According to the Wenzel model, the hydrophilicity of a surface is affected by both

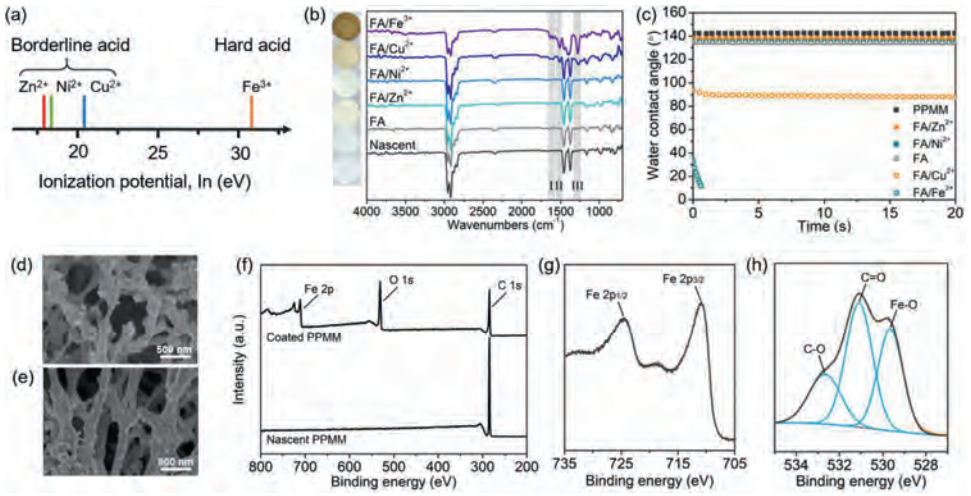

Fig. 2. (a) Ionization potential of various transition metal ions used in this work [42]. (b) Digital photographs, ATR-FTIR spectra, and (c) dynamic water contact angles of nascent and modified PPMMs (deposition conditions: pH 5.0, FA/metal salt = 1:1, FA = 2.0 mg/mL, deposition time of 12 h). SEM images of (d) the nascent and (e) the FA/Fe^{3+}-coated PPMM. XPS spectra of the FA/Fe^{3+}-coated PPMM: (f) survey, (g) Fe 2p and (h) O 1s.

surface chemistry and surface roughness [45,46]. Thus, the existence of both hydrophilic FA/Fe^{3+} coating and the micro/nano surface structure endows the membrane with superhydrophilicity.

XPS spectra also demonstrate the presence of O and Fe elements in the coated membrane (Fig. 2f). Two peaks at around 712 eV and 720 eV represent signals of Fe $2p_{3/2}$ and Fe $2p_{1/2}$, respectively, indicating Fe^{3+} is the main specie of Fe element (Fig. 2g). The signal of O 1s can be divided into three peaks at around 539.6, 531.1 and 532.7 eV, which can be assigned to Fe−O, C=O and C−O, respectively (Fig. 2h). The signal of Fe−O further confirms the coordination interaction between Fe^{3+} and FA [43,47].

The stability of the FA/Fe^{3+} coatings towards various organic solvents, acid, and alkaline solutions has been studied. As shown in Fig. S6a (Supporting information), after immersed in various organic solvents for 24 h at room temperature, the color of the leaching solutions and the membranes remain almost unchanged. UV-vis spectra show trace amount of extractives, indicating excellent stability of the coatings towards the studied organic solvents (Fig. S8b in Supporting information). In the range of pH 3.0~9.0, the concentration of the extractives is very low. However, when pH value is lower than 3.0 or higher than 9.0, the coatings may disaggregate (Fig. S9 in Supporting information). In fact, pH-responsiveness is a feature of metal-phenol complexes, which enables them to be applied in drug delivery system and other fields [16,20].

The surface wettability of polymer membranes is crucial to the applications in oil/water separation [48–50]. As shown in Fig. 3a, after prewetted by water, the underwater oil contact angles of the FA/Fe^{3+}-coated PPMMs towards various heavy and light oils are all above 150°, indicating excellent underwater super-oleophobicity and great potentials in oil/water separation [48,51].

In the oil/water mixture separation, three different kinds of light oils (*i.e.*, *n*-octane, petroleum ether and toluene) were used. During the separation, water can permeate through the coated PPMM, whereas *n*-octane (dyed red) is isolated above the membrane (Fig. 3b). The studied oil/water mixtures are successfully separated by the coated membrane with separation efficiencies all above 99% (Fig. 3c). The membranes can be used repeatedly, and each separation cycle takes about 18 min for the first 10 cycles of separation (Fig. S10 in Supporting information).

In the oil/water emulsion separation experiments, five different emulsions, including both light and heavy oils, were taken into investigation (Fig. S11 in Supporting information). Taking petroleum ether-in-water emulsion as an example, after filtrated by the coated PPMM, the clear and transparent filtrate of water is separated from the red milky surfactant-stabilized feed emulsion (Fig. 3d). For all oil-in-water emulsions, the total organic carbon (TOC) test results show that the separation efficiencies are all above 99%, and the fluxes are all higher than 140 LMH (Fig. 3e). Moreover, during 10 cycles of emulsion separation, there is no significant decline in both flux and separation efficiency (Fig. 3f).

The surface of FA/Fe^{3+}-coated membrane is positively charged at pH between 3.0 and 9.0 (Fig. 4a), making it potential for anionic dye adsorption via electrostatic interaction [52]. The direct red 80 aqueous solution was taken as an example. After permeating through the coated PPMM, the red solution turns into colorless, while the coated membrane adsorbs the dye and its color changes from initial brown to red (inset in Fig. 4b). UV-vis spectrum shows that the dye concentration is almost negligible in the filtrate, demonstrating the high removal efficiency.

The adsorption capacity towards various anionic dyes increases with the molecular weight and charge of the dyes (Fig. 4c, Figs. S12, S13 and Table S6 in Supporting information), reaching 0.25, 0.23, 0.10 and 0.03 mg/cm^2 for direct red 80, direct yellow 80, methyl blue, and methyl orange, respectively. The removal efficiencies are all above 99%. Besides, the positive surface charge of the coated membranes decreases with the pH value of the solutions (Fig. 4a and Fig. S14 in Supporting information), and the adsorption capacity decreases correspondingly (Fig. 4d). At the same time, it is reasonable that the modified membrane can barely adsorb cationic dyes (Fig. S15 in Supporting information).

The above-mentioned results demonstrate that the adsorption process is mainly driven by the attractive electrostatic interaction between the positively-charged membranes and the negatively-charged dyes. Therefore, the FA/Fe^{3+}-coated membrane may have the potential to separate the mixture of anionic and cationic dyes by selectively adsorbing the anionic dyes. The mixture solution of methylene blue (MeB, cationic) and direct yellow 50 (DY, anionic) was prepared, which turns to blue (the original color of MeB solution) after being filtrated (Fig. 4e). UV-vis spectra also confirm the selective adsorption of negatively-charged dyes (Fig. 4f). The absorption peak of DY at ~430 nm disappears after filtration, which means the anionic DY molecules have been almost fully removed from the mixture. Moreover, MeB molecules that are positively charged can interact with DY molecules and form black precipitates on the membrane surface (Fig. S16 in Supporting informa-

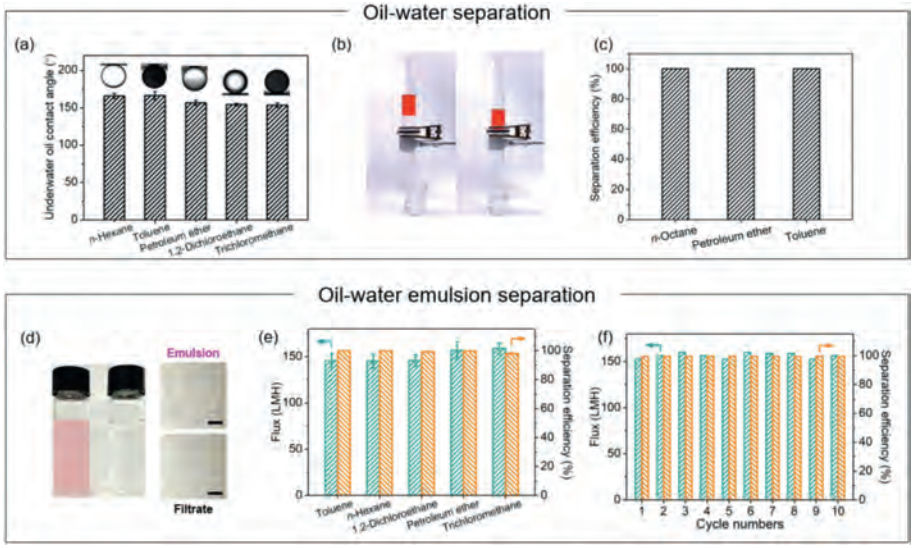

Fig. 3. Performance of the coated PPMM in oil/water separation. (a) Underwater oil contact angles towards different oils. (b) Digital photographs of the separation setup incorporating the coated PPMM in the middle. (c) Separation efficiency of different oil/water mixtures. (d) Digital and optical photographs of the emulsion and filtrate. Scale bar: 50 μm. (e) Fluxes and separation efficiencies of different oil-in-water emulsions. (f) Long-term performance of the coated PPMM for petroleum ether-in-water emulsion separation.

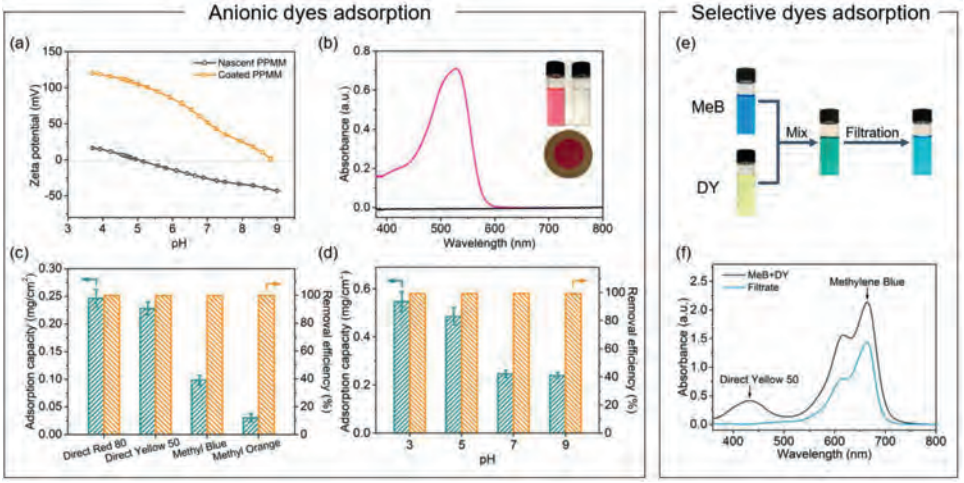

Fig. 4. Performance of the FA/Fe^{3+}-coated PPMM in anionic dyes adsorption. (a) Zeta potential of the nascent and coated PPMM at various pH values. (b) UV-vis spectra of the dye solution of direct red 80 and the corresponding filtrate. Insets: digital photographs of the feed and filtrate solutions, and the membrane after filtration. (c) Adsorption capacity and removal efficiency of the coated PPMM toward different dyes. (d) Adsorption capacity and removal efficiency of the coated PPMM toward direct red 80 solution of different pH values. (e) Digital photographs and (f) UV-vis spectra of MeB/DY mixture before and after filtration.

tion), which slightly decreases the concentration of MeB in the filtrate (~660 nm, Fig. 4f) and leads to the change in the solution color (Fig. 4e).

In conclusion, we propose a simple, fast, and effective method to fabricate monophenol-based MPNs. Effects of metal ions (Cu^{2+}, Zn^{2+}, Ni^{2+}, and Fe^{3+}) on the surface deposition demonstrate that the Fe^{3+} ions with stronger electron acceptability are conducive to the formation of MPNs with FA, and significantly reduce the deposition time to only 40 min from generally 24 h. Other deposition parameters such as pH and ligand-to-metal mass ratio have also been investigated. The results indicate that the formation of FA/Fe^{3+} coatings is controlled by the combination effect of FA/Fe^{3+} coordination, Fe^{3+} hydrolysis, and FA deprotonation. The FA/Fe^{3+} coatings endow the PPMM with underwater superoleophobicity, which makes the membranes applicable to the separation of oil/water mixtures and emulsions with high separation efficiency and excellent long-term stability. Moreover, the coated membranes are highly positively charged, which can adsorb anionic dyes and separate them from cationic dyes. Furthermore, taking the advantage of the time-saving and controllable process, FA/Fe^{3+} MPNs can be introduced to other fields such as drug delivery system and nanofiltration.

Declaration of competing interest

The authors declare that they have no known competing financial interests or personal relationships that could have appeared to influence the work reported in this paper.

Acknowledgments

Financial support from the National Natural Science Foundation of China (No. 51873192) and Zhejiang Provincial Natural Science Foundation of China (No. LZ20E030002) is gratefully acknowledged.

Supplementary materials

Supplementary data associated with this article can be found, in the online version, at doi:10.1016/j.cclet.2021.05.023.

References

[1] D.J. Miller, D.R. Dreyer, C.W. Bielawski, et al., Angew. Chem. Int. Ed. 56 (2017) 4662–4711.
[2] I. Banerjee, R.C. Pangule, R.S. Kane, Adv. Mater. 23 (2011) 690–718.
[3] M. Cloutier, D. Mantovani, F. Rosei, Trends Biotechnol. 33 (2015) 637–652.
[4] S. Kalluri, M. Yoon, M. Jo, et al., Adv. Mater. 29 (2017) 1605807.
[5] O. Garcia-Valdez, P. Champagne, M.F. Cunningham, Prog. Polym. Sci. 76 (2018) 151–173.
[6] N. Meyerbroker, T. Kriesche, M. Zharnikov, ACS Appl. Mater. Interfaces 5 (2013) 2641–2649.
[7] W. Xu, M. Niu, X. Yang, et al., Chin. Chem. Lett. 32 (2020) 489–492.
[8] D. Li, Y.N. Xia, Adv. Mater. 16 (2004) 1151–1170.
[9] G. Decher, Science 277 (1997) 1232–1237.
[10] W. Chen, H.D. Tang, Y.L. Chen, et al., Nano Energy 78 (2020) 11.
[11] J.H. Feng, S. Xiong, Z.G. Wang, et al., J. Membr. Sci. 550 (2018) 246–253.
[12] H.C. Yang, R.Z. Waldman, M.B. Wu, et al., Adv. Funct. Mater. 28 (2018) 1705327.
[13] Z.X. Wang, H.C. Yang, F. He, et al., Matter 1 (2019) 115–155.
[14] S.F. Zhao, M. Golestani, A. Penesyan, et al., Chin. Chem. Lett. 31 (2020) 851–854.
[15] W.M. Zhong, Y.Y. Zhang, L. Zhao, et al., Chin. Chem. Lett. 31 (2020) 2651–2656.
[16] H. Ejima, J.J. Richardson, K. Liang, et al., Science 341 (2013) 154–157.
[17] H. Ejima, J.J. Richardson, F. Caruso, Nano Today 12 (2017) 136–148.
[18] Q.Z. Zhong, S.Y. Li, J.Q. Chen, et al., Angew. Chem. Int. Ed. 58 (2019) 12563–12568.
[19] H. Lee, S.M. Dellatore, W.M. Miller, et al., Science 318 (2007) 426–430.
[20] J.L. Guo, Y. Ping, H. Ejima, et al., Angew. Chem. Int. Ed. 53 (2014) 5546–5551.
[21] D.D. Li, H. Shen, C. Cai, et al., ACS Omega 2 (2017) 1738–1745.
[22] J.D. Chen, H.Y. Wang, Y.T. Gong, et al., J. Mater. Chem. A 7 (2019) 11038–11043.
[23] F.J. You, Y.C. Xu, X.B. Yang, et al., Chem. Commun. 53 (2017) 6128–6131.
[24] Q. Dai, Q. Yu, Y. Tian, et al., ACS Appl. Mater. Interfaces. 11 (2019) 29305–29311.
[25] E. Filippidi, T.R. Cristiani, C.D. Eisenbach, et al., Science 358 (2017) 502–505.
[26] N. Holten-Andersen, M.J. Harrington, H. Birkedal, et al., P. Natl. Acad. Sci. U. S. A. 108 (2011) 2651–2655.
[27] Q. Ye, F. Zhou, W.M. Liu, Chem. Soc. Re. 40 (2011) 4244–4258.
[28] S. Quideau, D. Deffieux, C. Douat-Casassus, et al., Angew. Chem. Int. Ed. 50 (2011) 586–621.
[29] B.A. Acosta-Estrada, J.A. Gutierrez-Uribe, S.O. Serna-Saldivar, Food Chem. 152 (2014) 46–55.
[30] M.A. Rahim, K. Kempe, M. Mullner, et al., Chem. Mater. 27 (2015) 5825–5832.
[31] M.A. Rahim, M. Bjornmalm, T. Suma, et al., Angew. Chem. Int. Ed. 55 (2016) 13803–13807.
[32] N. Bertleff-Zieschang, M.A. Rahim, Y. Ju, et al., Chem. Commun. 53 (2017) 1068–1071.
[33] M.A. Rahim, M. Bjornmalm, N. Bertleff-Zieschang, et al., Adv. Mater. 29 (2017) 1606717.
[34] M.A. Rahim, M. Bjornmalm, N. Bertleff-Zieschang, et al., ACS Appl. Mater. Interfaces 10 (2018) 7632–7639.
[35] D.K. Yeon, S.H. Ki, J. Choi, et al., Langmuir 33 (2017) 3639–3646.
[36] H. Yu, Q.Z. Zhong, T.G. Liu, et al., Langmuir 35 (2019) 3643–3650.
[37] T. An, H. Yu, L.J. Xu, et al., Acta Polym. Sin. 50 (2019) 1298–1304.
[38] Q.Z. Zhong, J.J. Richardson, A.I. He, et al., Angew. Chem. Int. Ed. 60 (2021) 2346–2354.
[39] J. Yu, Y.J. Kan, M. Rapp, et al., Proc. Natl. Acad. Sci. U. S. A. 110 (2013) 15680–15685.
[40] Q.Z. Zhong, S.J. Pan, M.A. Rahim, et al., ACS Appl. Mater. Interfaces. 10 (2018) 33721–33729.
[41] R.G. Pearson, J. Am. Chem. Soc. 85 (1963) 3533–3539.
[42] X.D. You, H. Wu, R.N. Zhang, et al., Nat. Commun. 10 (2019) 581–587.
[43] M.A. Rahim, H. Ejima, K.L. Cho, et al., Chem. Mater. 26 (2014) 1645–1653.
[44] A.K. Jordao, M.D. Vargas, A.C. Pinto, et al., RSC Adv. 5 (2015) 67909–67943.
[45] R.N. Wenzel, Ind. Eng. Chem. 28 (1936) 988–994.
[46] M.J. Liu, S.T. Wang, L. Jiang, Nat. Rev. Mater. 2 (2017) 4160.
[47] J.F. Moulder, J. Chastain, R.C. King, Chem. Phys. Lett. 220 (1992) 7–10.
[48] Y.B. Wei, H. Qi, X. Gong, et al., Adv. Mater. Interfaces. 5 (2018) 1800576.
[49] Z. Xiong, Z.J. He, S. Mahmud, et al., ACS Appl. Mater. Interfaces 12 (2020) 47018–47028.
[50] X.L. Wang, Y.M. Pan, H. Yuan, et al., Chin. Chem. Lett. 31 (2020) 365–368.
[51] M. Zhu, Y.C. Liu, M.Y. Chen, et al., Chin. Chem. Lett. 31 (2020) 2683–2688.
[52] W.Z. Qiu, H.C. Yang, L.S. Wan, et al., J. Mater. Chem. A 3 (2015) 14438–14444.